Kütahya Dumlupınar University
Institute of Graduate Studies

Journal of Scientific
Reports-A
E-ISSN: 2687-6167
Number 53, June 2023

RESEARCH ARTICLE

A NEW FORCE MEASUREMENT MECHANISM IN WIND TUNNEL: CFD AND EXPERIMENTAL VALIDATION ON A CYLINDER

Seda KIRMACI ARABACI[1*], Emre KİRAZ[2]

[1] Manisa Celal Bayar University, Mechanical Engineering Department, Manisa, seda.kirmaci@cbu.edu.tr, ORCID: 0000-0001-8903-5952
[2] Manisa Celal Bayar University, Mechanical Engineering Department, Manisa, emre.kiraaz@gmail.com, ORCID: 0000-0003-1524-2865

Receive Date:08.02.2023 *Accepted Date: 06.03.2023*

ABSTRACT

Wind tunnel tests are experiments carried out in private and state-supported institutions, which are of great importance for studies in aerodynamics. Wind tunnels are essential in the defense industry, the automotive industry, and even the construction industry. In this study, a force sensor holder (FSH), in the open subsonic wind tunnel test room is designed, and it is made to measure angled structures, angled prototypes, and especially for wings. The critical angles of wings and the angles of attack are necessary, especially regarding aerodynamic performance. This force sensor holder can be adjusted at 0-90 degree angles and used experimentally. After holder manufacturing, experiments and CFD analysis are carried out at a 0 degree angle on the cylinder body. This study conducts a Computational Fluid Dynamics (CFD) analysis using Realizable k-ε, and SST k-ω turbulence models. In this study, the accuracy of the CFD analysis of the drag coefficient on a cylinder is evaluated through a comparison with both experimental and literature data. The results revealed that the CFD analysis has a deviation of 5,11% (using the Realizable k-ε model) and 5,22% (using the SST k- ω model) from the literature data. On the other hand, the experimental results show a discrepancy of 3,77% compared to the literature data. These findings demonstrate the effectiveness of the CFD analysis in predicting drag coefficients and highlight the importance of validating such simulations with experimental data.

Keywords: *Wind tunnel, Force sensor holder, Drag coefficient, Angle of attacks.*

1. INTRODUCTION

Aerodynamic forces can be calculated with wind tunnels used in academic and sectoral studies. The Aerodynamic forces that depend on speed and exterior body design can be calculated in computational fluid analysis programs and wind tunnels in inland vehicles. By examining the aerodynamic properties of aircraft such as airplanes, unmanned aerial vehicles, helicopters, balloons, parachutes, and land vehicles such as cars, trucks, buses, and motorcycles, fuel savings, and forces can be examined. In buildings such as high buildings, towers, and bridges, the wind tunnel's airflow effects, the strengths

of the storm, and their results can be investigated. In addition, wind turbine blades, jet blades, and speedboat forces can be calculated in wind tunnels. Ariyani et al. designed a model holder system in an open subsonic wind tunnel, and this holder is aimed to be dynamic, with three angular motions containing target seeking and wobbling [1]. Behavior tests of external objects can be performed more reliably as the aircraft model must be simulated based on the force and angular measurement between the external object [2]. A wind tunnel's force sensor and sensor holding are crucial measurement tools [3]. A balance rig is an instrument that measures the needed moment and forces of the prototype in the wind tunnel. Balance is divided into two; external and internal [4]. Computational Fluid Dynamics (CFD) is used as a verification method in wind tunnel applications. It is influential in creating suitable parameters for wind tunnels in CFD [5]. Gebel et al. conducted on the vehicles, and it was found that the datas in the wind tunnel and CFD were close and consistent between 0,75% and 7,40% [6]. Five different turbulence models are studied to find the most suitable model [7].

The force balance provided by internal and external balancing systems and load balancing systems made with complex and expensive components makes wind tunnel force measurement expensive and complicated. In addition, due to the non-standardization of materials, in case of any deformation, all production processes, from design to analysis, from production to quality control, require the production of parts by repeating, creating great difficulties in terms of time, operation, and finance. In addition, no force measurement mechanism in the domestic/foreign market can take measurements at different angles of attack/different angles while the prototype is positioned in a fixed position.

Experiments with force measurement mechanisms of wind tunnels will be more straightforward and give reliable results with this force sensor holder (FSH). This mechanism, which is durable and does not require constant adjustment, will be preferred over competitors. This invention's use of the wind tunnel will be made easier and more accessible with all these advantages provided. The invention aims to present a force measurement mechanism in which force measurement can be achieved by holding the test prototype at different angles to the airflow and the floor of the test chamber. The acceptability of the results are confirmed with experimental and CFD analyses on a cylinder body with L(length)/D(diameter)=2 (the literature supports) at 0 degrees. The aim of this study is to design a holder for a force sensor that can measure drag force at various angles for use in wind tunnels. Using this holder, a study was conducted on a cylinder at a 0-degree angle to measure drag force at different angles.

2. MATERIALS AND METHODS

In this part, a new Force Sensor Holder used in the wind tunnel mechanism is investigated. This force sensor holder can be adjusted at 0-90 degrees angles and used experimentally.

2.1. The Mechanism of FSH

The force sensor holder mechanism is adapted for the Wind Tunnel test room of Manisa Celal Bayar University, and this mechanism has been made available for all wind tunnels. Instead of preparing a separate experimental setup for each prototype, the mechanism is designed to apply to all prototypes. The primary condition for obtaining efficient and accurate data in wind tunnel tests is to develop the experimental setup so that it is not affected by the forces of the mechanism or other external factors.

The designed force sensor holder can measure the holding force without loss. It is to enable the experiments of prototypes at all desired angles and positions in the investigations of the Defense Industry, Automotive Industry, Civil Aviation, and Wind Energy and to provide the opportunity to find the desired aerodynamic forces. Moreover, this design is aimed to reduce costs compared to mechanisms that take measurements with other holders. A restrained force measurement mechanism that can move at different angles, which is the subject of the invention, is the essential component of the wind tunnel in terms of the accuracy and reliability of the data to be obtained from the wind tunnel. It moves at different angles, especially unmanned aerial vehicle wing structures. It is a great privilege to be used in models where the angle of attack is essential. As a result of the wind tunnel experiment calculations, the drag (C_D) and the lift (C_L) coefficients can be calculated. Defining the values of aerodynamic performance (C_L / C_D) at different angles will provide a tremendous advantage for experimental calculations.

Moreover, the fact that it can be done at a low cost will enable much better than other holders. The C_L/C_D values obtained by experimental studies with this holder will be able to analyze the changes with the angle of attack and free flow velocity. The FSH is located in the center of the Wind Tunnel test chamber and positioned to be mounted from the prototype's center of gravity.

It has been designed by mounting on the prototype to avoid creating any rolling moment, pitching moment, or yaw moment that will occur, especially in the axis. By opening two channels on the prototype, the assembly process will be ensured and connected to all kinds of prototypes with the help of bolts through these channels. The invention is a force measurement mechanism for holding the test component inside the wind tunnel for aerodynamic tests by exposing it to airflow in a wind tunnel where airflow is provided. The holder (Figure 1), which provides the fixation of the test piece, can ensure that the two extensions are connected from a support point and that the test component is held at different angles according to the airflow. Moreover, it has freedom of rotation about the support point. (Figure 1(a)-number 2 and detail figure in Figure 1(b)). It includes at least one fixing element to ensure the extensions are fixed after adjusting the angle between them. In addition, this mechanism consists of a sensor to measure force. (Figure 1(a)-number 4). A force measuring mechanism includes a sensor holder with a sensor slot for holding the sensor and connecting it to the test part. Moreover, a cable channel is configured so the cable providing power transmission to the sensor can be positioned. (Figure 1(a)-number 3). The sensor holder; includes a cable channel cover (Figure 1(a)-number 5) that enables the sensor slot to form an isolated volume from the external environment. The others parts in Figure 1(a) are the bolts and the screw pins.

JSR A
Journal of Scientific Reports

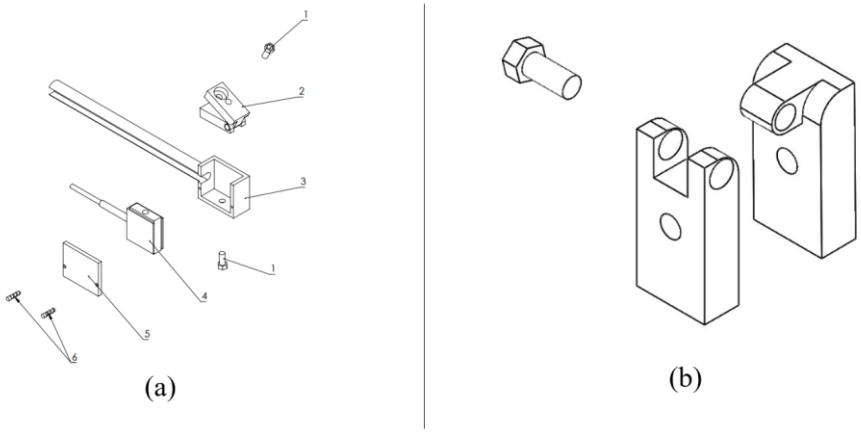

Figure 1. The force sensor holder (a) the Mechanism of FSH (b) number 2 detail of FSH in 'Figure 1.a'.

Depending on the direction, the prototype can yield results for both vertical and horizontal forces when the force sensor is mounted onto the mechanism. Force measurement mechanisms created with complex balancing systems are expensive and difficult to use. The first condition to get correct results in a wind tunnel is to neutralize internal and external loads. While testing the aerodynamic forces of the test prototype, it is of great importance that the test system does not affect these loads and that the weights of the prototype and the test mechanisms are balanced. The wind tunnel's work area needs three degrees of kinematic rotational motion. The planned angular motion is 00-900 for the pitch link. The yaw, pitch, and roll rotations are shown in Figure 2. In the study, the angle of pitch rotation is designed for wings.

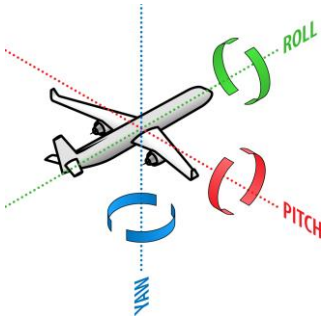

Figure 2. Yaw, pitch, and roll rotations of a plane.

In this study, a holder that can change the pitch rotation angle and take a smooth and accurate measurement in the x-axis direction is designed. It is planned that the place of use will be mainly the wings.

JSR A
Journal of Scientific Reports

2.2. Calculating Drag and Lift

The effect that the force applied to an object in a fluid will create in the opposite direction is called the drag force. The drag coefficient, the essential property among the parameters in the drag force, is a dimensionless number displayed as C_D (Eq. 1). ρ; is the density of the fluid, V; is the velocity of the fluid, and A; is the cross-sectional area perpendicular to flow.

$$C_D = \frac{F_d}{0.5\rho AV^2} \tag{1}$$

The value of the sensor on the axis of the wind speed vector in the experiment set will give the drag force. The measurement taken on the vertical axis will provide the lift force. Lift, for an airfoil, results from the surface forces generated by the fluid across the wing. When air flows around a wing at a specific velocity, a lower pressure is detected on the upper surface of the wing than on its lower surface.

The lift force is obtained if the pressure on the bottom surface is high. The lift force is denoted as F_L. The lift coefficient is one of the most critical parameters in the lift force. The lift coefficient is also dimensionless and defined as C_L (Eq. 2).

$$C_L = \frac{F_l}{0.5\rho AV^2} \tag{2}$$

The angle of attack is the angle between the relative motion vectors between the fluid and the reference line on the body. The angle of attack affects the lift coefficient of the airplane. The plane is observed at critical angles in a stalled state. The plane's stall depends on the air speed, the plane's weight, and the plane's center of gravity. Critical angles of attack are 15-18 degrees on most wings [8]. The newly invented force sensor holder will enable measurements to be taken up to 90 degrees. (Figure 1).

3. CFD METHOLOGY

Fluent software is used for the CFD solution and the boundary conditions used in the experiment are adapted to the CFD.

3.1. Governing Equations

The Navier-Stokes is utilized to model the flow of fluids. These equations include momentum equations and continuity, which are necessary for describing the movement of fluids. The three-dimensional, compressible, unsteady flow is represented by Eq. (3) and (4) derived from the Navier-Stokes equations. The continuity equation is written as follows:

$$\frac{\partial \rho}{\partial t} + \vec{\nabla}(\rho\vec{V}) = 0 \tag{3}$$

The Navier-Stokes equations is written as in x direction:

JSR A
Journal of Scientific Reports

$$\frac{\partial(\rho u)}{\partial t} + \nabla(\rho u V) = -\frac{\partial \rho}{\partial x} + \frac{\partial \tau_{xx}}{\partial x} + \frac{\partial \tau_{yy}}{\partial y} + \frac{\partial \tau_{zz}}{\partial z} + \rho f_x \quad (4)$$

3.2. Turbulence Model

3.2.1. SST k-ω turbulence model:

The shear stress transport (SST) k-ω turbulence model is a two-equation that combines the Standard k-ω model and the Standard k-ω model [9]. The model is well-suited for simulating complex turbulent flow fields that involve separation. However, achieving convergence in the analysis can be challenging and a proper mesh resolution near the wall is necessary, which can result in increased computational effort and power consumption. The SST k-ω turbulence model is calculated by (5) and (6) Eq.

$$\frac{\partial(\rho k)}{\partial t} + \frac{\partial(\rho u_j k)}{\partial x_j} = \tau_{ij}\frac{\partial U_i}{\partial x_j} - \beta^* \rho \omega k + \frac{\partial}{\partial x_j}\left[(\mu + \sigma_k \mu_t)\frac{\partial k}{\partial x_j}\right] \quad (5)$$

$$\frac{\partial(\rho \omega)}{\partial t} + \frac{\partial(\rho u_j \omega)}{\partial x_j} = \frac{\gamma}{v_t}\tau_{ij}\frac{\partial U_i}{\partial x_j} - \beta \rho \omega^2 + \frac{\partial}{\partial x_j}\left[(\mu + \sigma_k \mu_t)\frac{\partial \omega}{\partial x_j}\right] + 2(1 - \tanh(arg_1{}^4))\frac{\rho \sigma \omega_2}{\omega}\frac{\partial k}{\partial x_i}\frac{\partial \omega}{\partial x_j} \quad (6)$$

3.2.2. Realizable k-ε turbulence model:

The Realizable k-ε model is known for its performance in simulating boundary layers with rotation, adverse pressure gradients and recirculation. Additionally, it can accurately capture the flow of complex structures. The turbulence model is represented by Eq. (7) and (8) [10,11].

$$\frac{\partial(\rho k)}{\partial t} + \frac{\partial(\rho u_j k)}{\partial x_i} = \frac{\partial}{\partial x_j}\left[\left(\mu + \frac{\mu_t}{\sigma_k}\right)\frac{\partial k}{\partial x_j}\right] + P_k + P_b - \rho \varepsilon - Y_M + S_k \quad (7)$$

$$\frac{\partial(\rho \varepsilon)}{\partial t} + \frac{\partial(\rho u_j \varepsilon)}{\partial x_j} = \frac{\partial}{\partial x_j}\left[\left(\mu + \frac{\mu_t}{\sigma_\varepsilon}\right)\frac{\partial \varepsilon}{\partial x_j}\right] + \rho C_1 S_\varepsilon - \rho C_2 \frac{\varepsilon^2}{k + \sqrt{\vartheta \varepsilon}} + C_{1\varepsilon}\frac{\varepsilon}{k}C_{3\varepsilon}P_b + S_\varepsilon \quad (8)$$

P_k is the turbulence kinetic energy generation, P_b is the turbulence kinetic energy generation.

3.3. CFD Analysis

A cylinder body is designed with an aspect ratio of L/D=2 using NX. A rectangular control volume is created with a length ten times that of the body and a total height four times the body height. The mesh is generated four times starting from 82000 up to 330000. During the investigation of the drag coefficient, it was observed that the range at which the drag coefficient begins to remain constant starts from 300000 when examining the mesh values. Figure 3 shows the tetrahedral mesh.

JSR A
Journal of Scientific Reports

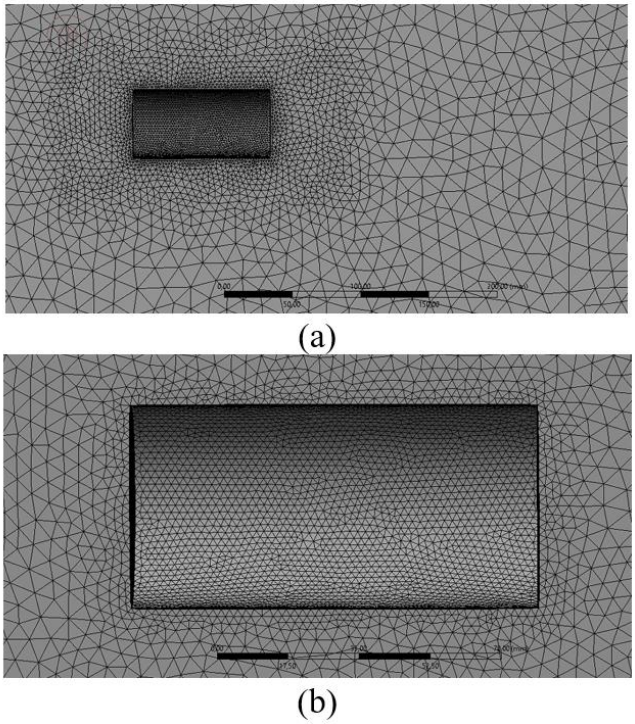

Figure 3. Tetrahedral Mesh of cylinder body a) around the body b) near the body wall.

The CFD solution is computed using Fluent software, with the solution method being chosen as second order upwind for the flow. The flow field is solved as a steady-state condition. The wall function is defined as enhancement wall treatment Realizable k-ε turbulences model. And the other turbulence model is selected SST k-ω model. First layer thickness also wall distance y is calculated as 1.8e-5 m when y^+=1; and Reynolds number of cylinder body is calculated as 1.3e+6.

4. EXPERIMENTAL METHODS

The wind tunnel test room at Manisa Celal Bayar University has a mechanism for measuring force. The dimensions of the test room are 1000 mm in length and 300 x 300 mm^2 in section. The wind tunnel (Figure 4) has a maximum flow velocity of 70 m/s and a distance of approximately 6400 mm. The weight of the wind tunnel is 400 kg, and it has a contraction ratio of 11.1 [12].

JSR A
Journal of Scientific Reports

Figure 4. Manisa Celal Bayar University wind tunnel.

The cylinder's drag coefficient and drag force are calculated as in Figure 5 with the new force sensor holder for 0^0 at pitch rotation; this drag value is verified in the literature.

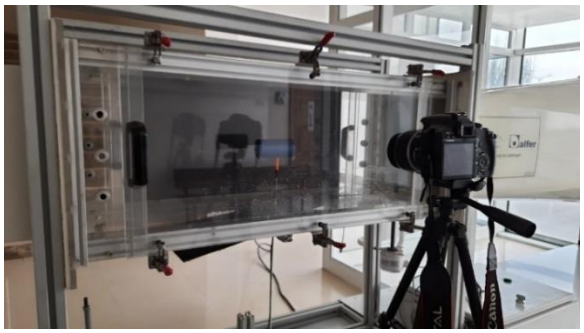

Figure 5. A cylinder body prototype (L/D=2).

5. RESULTS

This study presents a newly developed force sensor holder that is capable of moving at various angles, suitable for use in wind tunnel experiments. The cylinder body is tested using this newly developed force holder, and CFD analyses are conducted and compared with existing literature. The drag coefficient values obtained from the CFD solutions and experimental results are presented in Table 1 for each turbulence model. The differences between the results from the literature data and the experimental and CFD results are analyzed at a Reynolds Number of 94595. This paper calculates the drag coefficients at a speed of 28 m/s for both experimental and CFD results.

JSR A
Journal of Scientific Reports

Table 1. The results of drag coefficient for cylinder as L/D=2.

Results	**Drag coefficient** (C_d)	**Different (%)**
Experimental result	0,866	3,77%
k- ε Realizable (CFD)	0,854	5,11%
k-ω SST (CFD)	0,853	5,22 %
Çengel&Cimbala (2010) [9]	0,90	-

In the wind tunnel, the drag force is measured in the x direction at 0 degrees on the cylinder body. To validate the results, data from Çengel&Cimbala is taken into account. The drag coefficient values of the cylinder are determined when the drag force is calculated in the wind tunnel, and these values are attempted to be verified. The wind tunnel experimental results and literature results are presented in Table 1. The drag coefficient value of the cylinder is found to be 0,866 in the wind tunnel experiment, while it is 0,90 in the literature [13], 0,854 in the CFD analysis for the k-ε Realizable turbulence model, and 0,853 in the CFD analysis for the k-ω SST turbulence model.

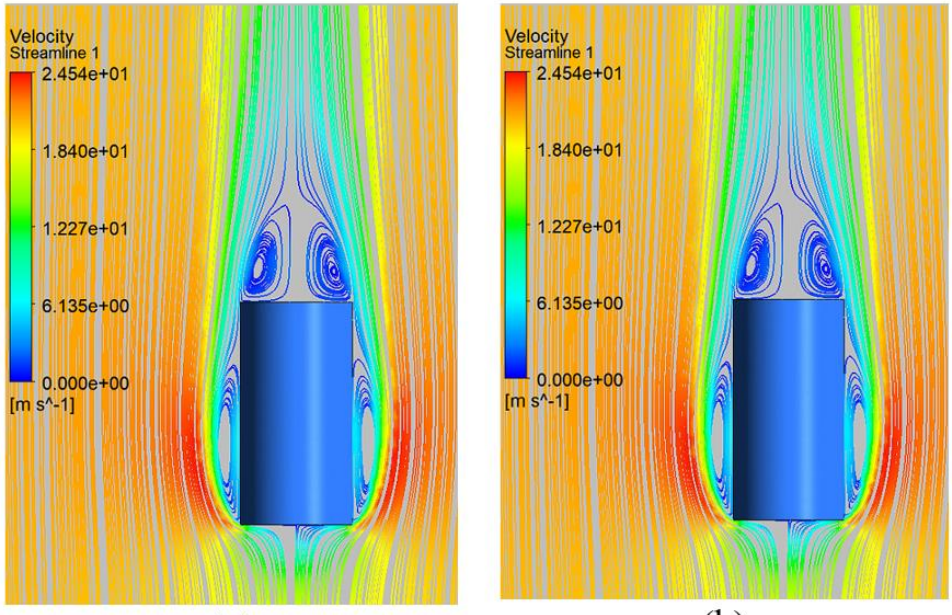

Figure 6. Velocity streamline on the cylinder body a) the realizable k- ε b) SST k-ω models.

Velocity streamlines are displayed in the rear of the cylinder model in Figure 6. It can be seen that a vortex forms in this area for both the Realizable k-ε and SST k-ω turbulence models.

JSR A
Journal of Scientific Reports

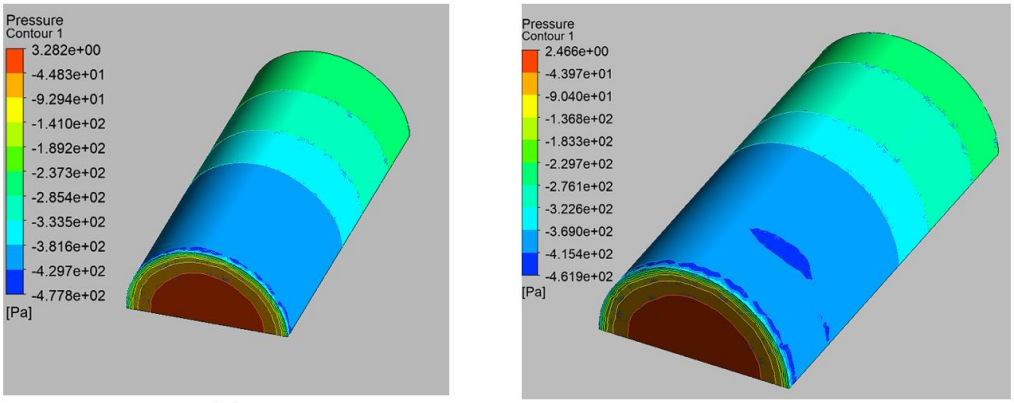

(a) (b)

Figure 7. Pressure contour of the cylinder body a) the realizable k- ε b) SST k-ω models.

Figure 7 presents the pressure contour of the cylinder body, which clearly shows a significant pressure difference between the front and rear regions for both turbulence models. The airflow behavior around a cylinder has been studied and observed to exhibit compression at the front of the cylinder, leading to a considerable increase in frontal pressure, as shown in Figure 7. The airflow moves smoothly along the body of the cylinder until it reaches the rear end, where it converges from various directions (top, bottom, and sides), creating a small vortex or flow recirculation at the rear end of the body. Due to the pressure difference, a considerable fraction of the overall drag force is experienced by the body.

The results of the study indicate that there is a deviation of 5,11% between the CFD analysis using the Realizable k-ε model and the literature data, and a deviation of 5,22% for the SST k-ω model, whereas the experimental results have a discrepancy of 3,77% when compared to the literature data. These results were calculated at a Reynolds number of 94595.

6. DISCUSSION AND CONCLUSION

This article presents the design and application of a new force sensor holder (FSH) for use in wind tunnel experiments. The FSH is designed to be frictionless, lossless, and innovative, allowing for stable and accurate measurements without being affected by moment forces. Its versatility and adaptability enable it to be mounted on various prototypes, measuring force at different angles.

An experimental study is conducted on a cylinder body (for L/D=2) at a 0 degree angle using the FSH. The results of the study matched the theoretical data, indicating that the FSH provided reliable data. The study is also compared with CFD analyses.

The findings indicated that the deviation of drag coefficient between the CFD analysis and literature data is 5,11% for the Realizable k-ε model and 5,22% for the SST k-ω model, while the experimental result has a discrepancy of 3,77% compared to the Çengel & Cimbala [13]. The differences between

the results in the literature data and the experimental and CFD results are given at 94595 Reynolds Number. The drag coefficients are calculated at 28 m/s in experimental and CFD results.

The FSH is intended for use mainly on wings in future studies, and it is planned to study wings from different angles. Overall, this new force sensor holder shows promise for providing accurate and reliable data in wind tunnel testing. Its frictionless and lossless design offers significant advantages over previous technologies, enabling accurate measurements of forces at different angles.

ACKNOWLEDGEMENT

The support of Manisa Celal Bayar University is highly appreciated. Funding Information: Manisa Celal Bayar University under project numbers BAP 2013-037.

REFERENCES

[1] Ariyani, N. R. and Nugroho, L., (2019). Conceptual design methodology of a 3-DOF Dynamic model holder system for open subsonic wind tunnel. IEEE International Conference on Aerospace Electronics and Remote Sensing Technology, ICARES, 1-7.

[2] Ulusal, N., (2005). Conceptual design of a model support system and its controller for Ankara wind tunnel, phD Thesis, Mechanical Engineering. Middle East Technical University, Ankara, Turkey, 1-119.

[3] Ahangar, M.R.H., Kangavari, M.R., and Vahedi, K. (2011). Reliability model of a wind tunnel balance system, Turkısh Journal of Engıneerıng and Envıronmental Scıences, 35, 21 – 30.

[4] Ahangar, M.R.H., Kangavari, M.R. and Berangi, R. (2006). Investigation of error sources on the balance and the standard dynamic model in the wind tunnel, ICAS Conference, Hamburg, Germany,1-9.

[5] Gonzalez, M., Ezquerro, J. M., Lapuerta, V., Laverón, A., and Rodríguez, J. (2011). Components of a wind tunnel balance: Design and calibration. Wind Tunnels and Experimental Fluid Dynamics Research, 1-20.

[6] Gebel, M. E., Önaldi, S., Korkmaz, S., Osmanoğlu, S., Özçelik, B., Ermurat, M. and İmal, M. (2018). Bir elektrikli aracin aerodinamik özelliklerinin deneysel ve sayisal olarak incelenmesi, 9th International Automotive Technologies Congress, Otekon, Bursa, Turkey, 850-858.

[7] Şumnu, A. (2021). Shape modification of Ahmed body to reduce drag coefficient and determination of turbulence model. Niğde Ömer Halisdemir University Journal of Engineering Sciences, 10(2), 824-832.

[8] https://fly8ma.com/topic/angle-of-attack-2/ (accessed date: 11.12.2022)

[9] Menter, F. R. (1994). Two-Equation Eddy-Viscosity Turbulence Models for Engineering Applications., AIAA journal., 32, 1598-1605.

[10] Wilcox, D.C. (1998). Turbulence modeling for CFD., La Canada, 2, 103-217.

[11] Fluent. (2009). ANSYS Fluent 12.0. Theory Guide. ANSYS Inc., Canonsburg, PA.

[12] Kırmacı Arabacı, S. and Pakdemirli, M., (2016). Improvement of aerodynamic design of vehicles with inspiration from creatures, PhD Thesis, Manisa Celal Bayar University, Manisa, 135s.

[13] Cengel, Y. and Cimbala, J., (2010). Fundamentals and Applications, McGraw-Hill (2nd Edition), 1006s.